

# Electrostatic shock waves in inhomogeneous plasmas with non-Maxwellian electron population.

Sara Zahoor

Physics Department,  
COMSATS Institute of Information and Technology,  
Islamabad, Pakistan  
sarazahoor360@gmail.com

**Abstract—** *The present work investigates the nonlinear electrostatic drift shock waves in inhomogeneous plasmas with non-thermal electrons. A theoretical construct has been shown that explains the formation of shocks in the Earth's ionosphere F layer. The plasma is assumed to be consisting of heavy ions and non-thermal electrons in which density inhomogeneity driven linear and nonlinear ion drift waves are investigated. Ion-neutral collision frequency introduces dissipation in the system. Making use of two nonthermal distributions i.e. kappa and Cairns distributions, we have derived the nonlinear Kadomtsev-Petviashvili (KP) Equation like equations in the small amplitude limit, and the solutions are obtained utilizing the tangent hyperbolic method. Using the plasma parameters typically found in the Earth's ionosphere, it is observed that the system under consideration admits rarefactive shocks. The characteristics of drift shock waves are found to be affected by the ion-neutral collision frequency, nonthermal electron population, inverse density inhomogeneity scalelength, and the ambient magnetic field.*

**Keywords;** *Drift shock waves, electrostatic shock potential, Cairns distribution, suprathermal particles.*

## I. INTRODUCTION

The ubiquitous presence of non-Maxwellian plasma population has been detected in the variety of space plasma environments by the space ventures from the last decades. They have been found to fit the observations and satellite data in the solar winds, magnetospheres, Earth's upper atmosphere etc. Since it is already well understood that drift shocks are formed in the presence of inhomogeneous magnetized plasma. The geometry is designed in such a manner that the ambient magnetic field ( $B_0\hat{z}$ ) is perpendicular to dynamical ion density, in addition to Boltzmann distributed inertialess electrons giving rise to electrostatic drift shock waves. Thus, the low-frequency (by comparison with the ion gyro frequency i.e.  $\Omega_{ci} = eB_0/m_i c$ ) waves having parallel (meaning along  $B_0$ ) phase velocity much smaller than the electron thermal velocity arise due to a balance between the time derivative density fluctuations and the  $(E \times B_0)$  convection of the unperturbed density.<sup>1</sup>

The physics of drift shocks has grown into a broader field of research and investigation as its applications descended from astrophysical heights to the terrestrial laboratory. At the laboratory level such plasma environment has been successfully created by Buchelnikova<sup>2</sup>, first theorizing the existence of drift solitary waves. Further the work was carried by Tasso<sup>15</sup>, Hendel *et al*<sup>3</sup> inspecting on the problem of temperature gradient and finally explained by Lakhin *et al*<sup>4</sup> by taking nonlinearity under consideration, in the absence of the temperature gradient. It was also shown that for the existence of the drift solitons, a sufficiently high level of the drift activity is necessary, which is characterized by the qualitative relation  $\frac{n}{n_0} \geq 1/k_{\perp} L_n$ , where

$n_0$  and  $\tilde{n}$  are the equilibrium and perturbed parts of the plasma number density,  $k_{\perp}$  is the characteristic transverse wave number of the soliton and  $L_n$  is the characteristic scale of inhomogeneity of the plasma number density.

It is known that shock waves can be excited in a dissipative nonlinear medium, here it is caused by the collisions between charged particles and neutrals present in the system. However, when a medium has both dispersive and dissipative properties, the propagation of small amplitude perturbations can then be adequately described by Korteweg-de Vries-Burgers (KdV) equation. The dissipative Burgers term in the nonlinear KdVB equation arises by taking into account the kinematic viscosity among the plasma constituents.<sup>5-7</sup>

When the wave breaking due to nonlinearity is balanced by the combined effect of dispersion and dissipation, a monotonic or oscillatory dispersive shock wave is generated in a plasma.<sup>12</sup> It is well known that transverse perturbations would always exist in the higher-dimensional system. The presence of transverse perturbation introduces anisotropy in the system which modifies the wave structure and the stability of the system.

Satellite probaton of ionosphere revealed that the F region has the highest concentration of free electrons and ions anywhere in the atmosphere. Above the F1 region, atomic oxygen becomes the dominant constituent because lighter particles tend to occupy at higher altitudes (at  $\sim 100$  km). This atomic oxygen provides the  $O^+$  atomic ions that make up the F2 layer<sup>8</sup>. Here a lot of interesting phenomena can occur. As the particles are partially ionized up there, so there is this fusion of electrons, ions and neutral atoms out there and all together their interactions can attenuate or strengthen the coherent structures, e.g. the dissipation is introduced in the system by the ion-neutral collision frequency.

W. Masood *et al*<sup>1</sup> briefly discussed the linear and nonlinear propagation of small amplitude drift shock waves in a plasma consisting of heavy ions and electrons (nonthermal<sup>9</sup>) using the drift approximation in a one dimensional (1-D) planar geometry. An extension of their work has been attempted by including the suprathermal plasma population<sup>10-11</sup> and upgrading up to three dimensional geometry. In this regard, Kadomtsev-Petviashvili-Burgers (KPB) equation is derived and its solution is presented using the tangent hyperbolic method<sup>13-14</sup>.

The present work is organized in the following manner: In Sec. (II), we present the governing set of equations for the problem under consideration and in Sec. (III) presents the linear dispersion relation. In Sec. (IV), we present the nonlinear analysis (Case A and Case B) whereas in C, the results are discussed. Finally, in Conclusion, the main findings of this paper has been recapitulate.

## II. MATHEMATICAL MODEL

Consider magnetized, inhomogeneous, and collisional plasma consisting of positive in addition to electrons and background neutral

particles. Ions are dynamical and assumed to have collisions with neutral particles. Let the external magnetic field consisting of oxygen ions of mass  $M_+$  ( $M_+ = 16m_p$ ) and electrons  $m_e$  respectively. The dynamics of low-frequency drift wave is then governed by the following set of equations:

Ion continuity equation,

$$\partial_t N_+ + \nabla \cdot (N_+ v_+) = 0$$

(1)

Equation of motion,

$$N_+ M_+ (\partial_t + (v_+ \cdot \nabla)) v_+ = q \left( E + \frac{1}{c} v_+ \times B_0 \right) - N_+ M_+ v_{n+} v_+$$

(2)

where  $N_+$ ,  $v_+$ ,  $q$  and  $v_{n+}$  represents the number density, fluid velocity, charge and neutral ion collisions, respectively. Making use of cold plasma approximation and quasi-neutrality condition i.e.  $\bar{n}_e \approx \bar{N}_+$  and take  $Z=1$ , since plasma is slightly charged. By resolving the components from the equation of motion, we obtain parallel component of velocity as,

$$(\partial_t + \partial_z v_+ + v_{n+}) v_{+||} = A_t v_{+||} = -\frac{q}{M_+} \partial_z \phi$$

(3)

and the perpendicular component is

$$v_{+\perp} \approx -\frac{c}{B_0} \nabla \phi \times \hat{z} - \frac{c}{\Omega_+ B_0} \frac{d}{dt} \nabla \perp \phi - \frac{c}{B_0} \frac{v_{n+}}{\Omega_+} \nabla \perp \phi$$

(4)

Whereas,  $v_E = \frac{c}{B_0} (\hat{z} \times \nabla \phi)$  is the electric drift velocity,  $v_p = \frac{c}{B_0} \frac{1}{\Omega_+} \partial_t \nabla \perp \phi$  is ion polarization velocity and  $v_c = \frac{c}{B_0} \frac{1}{\Omega_+} v_{n+} \nabla \perp \phi$  is ion collisional drift velocity.

Using the ion continuity equation, we have arrived at our model equation;

$$\frac{d}{dt} N_+ + \frac{c}{B_0} \hat{z} \times \nabla \phi \cdot \nabla N_+ - \frac{c N_+}{B_0 \Omega_+} \frac{d}{dt} \nabla \perp^2 \phi - \frac{c}{B_0 \Omega_+} N_+ v_{n+} \nabla \perp^2 \phi - \frac{q}{M_+} \partial_z \phi = 0$$

(5)

Here  $N_+$  is the total ion number density that contains both the unperturbed and the perturbed contributions.

R.A. Cairns *et al*\* showed that in the presence of non-thermal electron distribution, which are highly energetic, due to which the nature of ion sound solitary structures get modified and made possible to obtain such solutions with density depletion regions (cavitons). The total nonthermal electron number density is given as

$$\hat{n}_e = n_{e0} (1 - \beta \Phi + \beta \Phi^2) \exp(\Phi)$$

Where,  $\hat{n}_e$  is the electron density,  $n_{e0}$  is the electron density unperturbed,  $\beta$  is given by  $4Y/(1+3Y)$  and

where  $Y$  is a parameter, that determines the population of the non-thermal electrons.

For the sake of simplification, the normalized electron density can be written as

$$\bar{N}_+ = (1 - \beta) \Phi + \frac{1}{2} \Phi^2 = \Gamma \Phi + \frac{1}{2} \Phi^2,$$

(6)

On the other hand, a suprathermal population in space plasma follows quasi-Maxwellian distribution. Since the fast particles are nearly collision less in space plasmas, they are easily accelerated and tend to produce nonequilibrium velocity distributions functions with suprathermal tails decreasing as a power law of the velocity generally known as kappa distribution. Here the perturbed number density

$$\hat{n}_e = n_{e0} \left[ 1 - \frac{e\phi}{(k_e - \frac{3}{2}) T_e} \right]^{-(k_e - \frac{1}{2})}$$

For the sake of simplification, the normalized electron density can be written as

$$\hat{n}_e = n_{e0} (1 + \Gamma \Phi + \eta \Phi^2)$$

(7)

where  $\Phi = \frac{e\phi}{T_e}$ ,  $\Gamma = \frac{k-1}{k-\frac{3}{2}}$  and  $\eta = \frac{(k-\frac{1}{2})(k+\frac{1}{2})}{(k-\frac{3}{2})^2}$ .

Kappa distributions with  $2 < \kappa < 6$  have been found to fit the observations.

### III. DERIVATION OF KPB EQUATION

For localized solution, assuming a new coordinate with the variable  $\xi = k(y + az - ut)$  and making use of the distribution mentioned, following results are gained.

The simplified form,

$$\frac{\partial}{\partial \xi} \left[ \frac{\partial \phi}{\partial \xi} + A \phi \frac{\partial \phi}{\partial \xi} + B \frac{\partial^3 \phi}{\partial \xi^3} + C \frac{\partial^2 \phi}{\partial \xi^2} \right] + D \frac{\partial^2 \phi}{\partial \xi^2} = 0.$$

(8)

This is KP equation. Employing the tangent hyperbolic method the solution is

$$\phi(\xi) = \frac{-25B+3C^2-25\alpha^2AD}{50AB} + \frac{3C^2}{25AB} \tanh \xi - \frac{3C^2}{50AB} \tanh^2 \xi$$

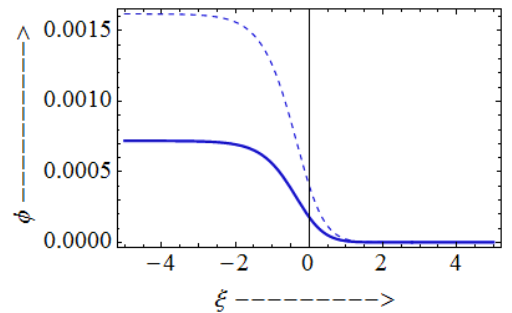


Fig. 1. At Variation of the electrostatic drift potential  $\Phi$  with varying Ion-neutral collision frequency,  $v_{n+} = 0.2$  Hz (Thick) and  $v_{n+} = 0.3$  Hz (Dashed).

### A. Case A

Using (5 and 6) the Cairns distribution, ion continuity equation can be rewritten as

$$\Gamma \frac{\partial \phi}{\partial t} + \phi \frac{\partial \phi}{\partial t} + v_+^* \frac{\partial \phi}{\partial y} \Gamma \phi + v_+^* \frac{\partial \phi}{\partial y} - \rho_+^2 \frac{\partial}{\partial t} \frac{\partial^2}{\partial y^2} \phi - \rho_+^2 v_{n+} \frac{\partial^2}{\partial y^2} \phi - \frac{q}{A_t M_+} \partial_z \phi = 0$$

For the localized solution, coordinate in the moving frame is assumed as  $\xi = k(y + \alpha z - ut)$ . Equation in the transformed frame is obtained as

$$\frac{\partial}{\partial \xi} \left[ \left( \Gamma - \frac{v_+^*}{u} \right) \frac{\partial \phi}{\partial \xi} + \left( 1 - \frac{v_+^* \Gamma}{u} \right) \phi \frac{\partial \phi}{\partial \xi} - (\rho_+^2) \frac{\partial^3 \phi}{\partial \xi^3} - \left( \frac{\rho_+^2 v_{n+}}{u} \right) \frac{\partial^2 \phi}{\partial \xi^2} \right] - \left( \frac{\alpha^2 c_s^2}{u^2} \right) \frac{\partial^2 \phi}{\partial \xi^2} = 0$$

where,

$$A_1 = \left( \Gamma - \frac{v_+^*}{u} \right), A_2 = 1 - \frac{v_+^* \Gamma}{u}, A_3 = -\rho_+^2, A_4 = \frac{\rho_+^2 v_{n+}}{u} \text{ and } A_5 = -\left( \frac{\alpha^2 c_s^2}{u^2} \right).$$

$$\text{Where } A = \left( \frac{1 - \frac{v_+^* \Gamma}{u}}{\left( \Gamma - \frac{v_+^*}{u} \right)} \right), B = \left( \frac{-\rho_+^2}{\left( \Gamma - \frac{v_+^*}{u} \right)} \right), C = \frac{\rho_+^2 v_{n+}}{\left( \Gamma - \frac{v_+^*}{u} \right) u} \text{ and } D = \left( \frac{-\left( \frac{\alpha^2 c_s^2}{u^2} \right)}{\left( \Gamma - \frac{v_+^*}{u} \right)} \right)$$

This yields equation (8) and correspondingly its solution is obtained as mentioned.

### B. Case B

This time utilizing kappa distribution (Equation 5 and 7) and the ion continuity equation takes the form

$$\Gamma \frac{\partial \phi}{\partial t} + \eta \phi \frac{\partial \phi}{\partial t} + v_+^* \eta \phi \frac{\partial \phi}{\partial y} + v_+^* \Gamma \frac{\partial \phi}{\partial y} - \rho_+^2 \frac{\partial}{\partial t} \frac{\partial^2}{\partial y^2} \phi - \rho_+^2 v_{n+} \frac{\partial^2}{\partial y^2} \phi - \frac{q}{A_t M_+} \partial_z \phi = 0$$

For the localized solution, coordinate in the moving frame is assumed as  $\xi = k(y + \alpha z - ut)$ . Equation in the transformed frame is obtained as

$$\frac{\partial}{\partial \xi} \left[ \left( \Gamma - \frac{v_+^*}{u} \right) \frac{\partial \phi}{\partial \xi} + \left( 2\eta - \frac{v_+^* \Gamma}{u} \right) \phi \frac{\partial \phi}{\partial \xi} - (\rho_+^2) \frac{\partial^3 \phi}{\partial \xi^3} - \left( \frac{\rho_+^2 v_{n+}}{u} \right) \frac{\partial^2 \phi}{\partial \xi^2} \right] - \left( \frac{\alpha^2 c_s^2}{u^2} \right) \frac{\partial^2 \phi}{\partial \xi^2} = 0$$

$$A_1 = \left( \Gamma - \frac{v_+^*}{u} \right), A_2 = 2\eta - \frac{v_+^* \Gamma}{u}, A_3 = -\rho_+^2, A_4 = \frac{\rho_+^2 v_{n+}}{u} \text{ and } A_5 = -\left( \frac{\alpha^2 c_s^2}{u^2} \right).$$

$$\text{Where } A = \left( \frac{2\eta - \frac{v_+^* \Gamma}{u}}{\left( \Gamma - \frac{v_+^*}{u} \right)} \right), B = \left( \frac{-\rho_+^2}{\left( \Gamma - \frac{v_+^*}{u} \right)} \right), C = \frac{\rho_+^2 v_{n+}}{\left( \Gamma - \frac{v_+^*}{u} \right) u} \text{ and } D = \left( \frac{-\left( \frac{\alpha^2 c_s^2}{u^2} \right)}{\left( \Gamma - \frac{v_+^*}{u} \right)} \right)$$

Once again this yields equation (8) and correspondingly its solution is obtained as mentioned.

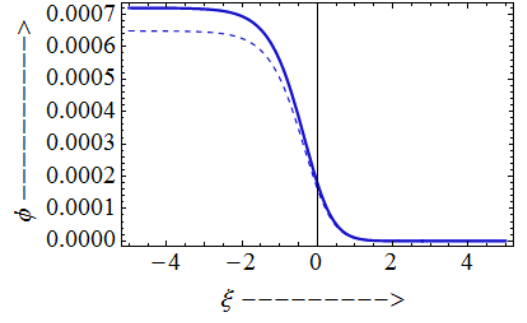


Fig.2. At Variation of the electrostatic drift potential  $\Phi$  with varying inverse scale length of density inhomogeneity  $\kappa_{ni} = 10^{-3}m$  (Thick) and  $\kappa_{ni} = 10^{-4}m$  (Dashed).

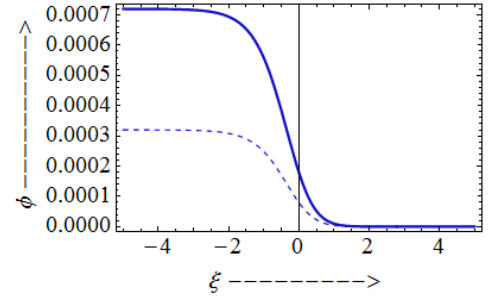


Fig.3. At Variation of the electrostatic drift potential  $\Phi$  with varying magnetic field  $B_0 = 0.2 G$  (Thick) and  $B_0 = 0.3 G$  (Dashed).

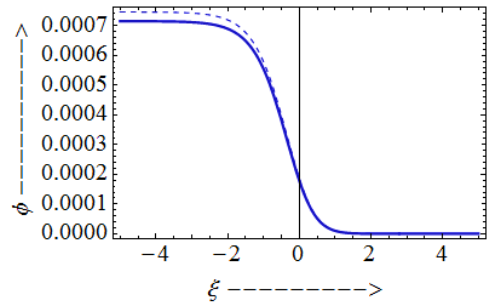


Fig.4. At Variation of the electrostatic drift potential  $\Phi$  with varying non-thermal ion population,  $\Gamma = 0.2$  (Thick) and  $\Gamma = 0.45$  (Dashed).

## IV. OBSERVATIONS.

For case **A**, it is observed from figure 1, that by increasing the collisional frequency the drift shock potential is increased. Figure 2 investigates the effects of increasing inverse scale length of density inhomogeneity, which decreases the shock potential. Similarly increasing magnetic field will attenuate the drift shock potential shown by figure 3. Whereas figure 4 is showing an increase in the potential due to increase in non-thermal ion population. For case **B**, by increasing non-thermal ion population and ion-neutral collisional frequency the shock potential is also found to be increased,

represented by figure 5 and 6. Furthermore increasing magnetic field will deteriorate the drift shock potential (figure 7). Lastly figure 8 investigates the effects of increasing inverse scale length of density inhomogeneity, which increases the shock potential.

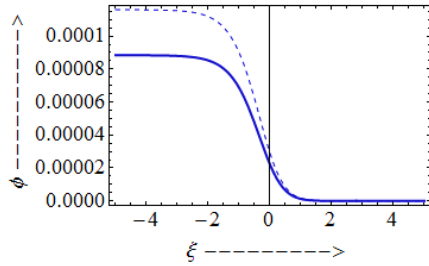


Fig.5. At Variation of the electrostatic drift potential  $\phi$  with varying non-thermal ion population,  $\kappa = 3$  (Thick) and  $\kappa = 3.5$  (Dashed).

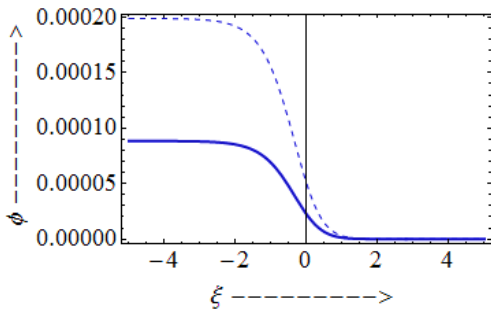


Fig.6. At Variation of the electrostatic drift potential  $\phi$  with varying Ion-neutral collision frequency,  $\nu_{n+} = 0.2 \text{ Hz}$  (Thick) and  $\nu_{n+} = 0.3 \text{ Hz}$  (Dashed).

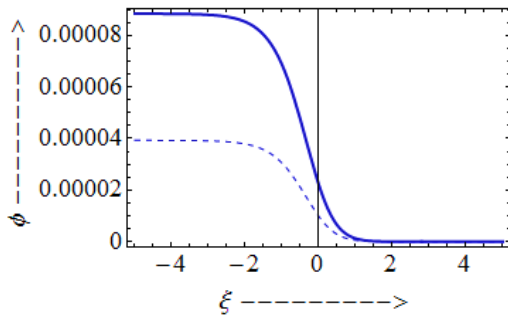


Fig.7. At Variation of the electrostatic drift potential  $\phi$  with varying magnetic field  $B_0 = 0.2 \text{ G}$  (Thick) and  $B_0 = 0.3 \text{ G}$  (Dashed).

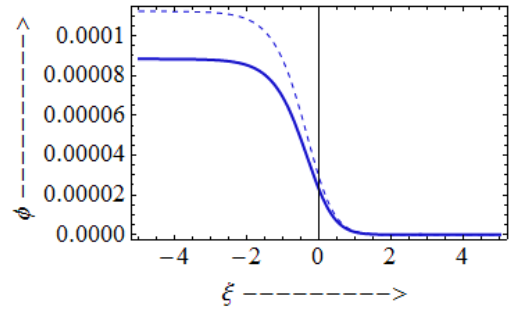


Fig.8. At Variation of the electrostatic drift potential  $\phi$  with varying inverse scale length of density inhomogeneity  $\kappa_{ni} = 10^{-3} \text{ m}$  (Thick) and  $\kappa_{ni} = 4 \times 10^{-3} \text{ m}$  (Dashed).

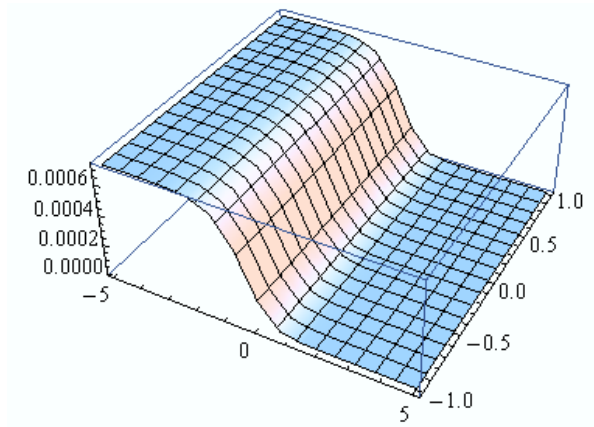


Fig.9. 3-D view of electrostatic drift potential for Case A

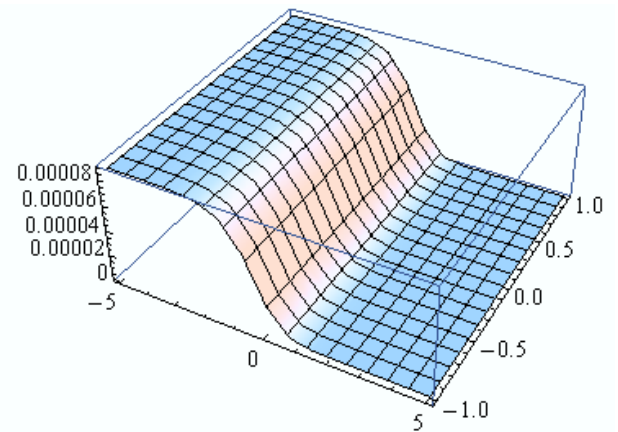


Fig.10. 3-D view of electrostatic drift potential for Case B

### I. DERIVATION OF KDVB EQUATION

Now when only perpendicular components were considered and parallel components were ignored, the model equation is derived as

$$\frac{d}{dt}N_+ + \frac{c}{B_0}\hat{z} \times \nabla\varphi \cdot \nabla N_+ - \frac{cN_+}{B_0\Omega_+} \frac{d}{dt}\nabla_{\perp}^2\varphi - \frac{c}{B_0\Omega_+}N_+v_{n+}\nabla_{\perp}^2\varphi = 0$$

For localized solution, here we choose an alternative coordinate with the variable  $\xi = k(y - ut)$  and making use of the distribution mentioned, Korteweg deVries-Burgers (KdVB) equation is obtained in the following form.

$$\frac{\partial\phi}{\partial\xi} + \frac{A}{2}\phi\frac{\partial\phi}{\partial\xi} + B\frac{\partial^3\phi}{\partial\xi^3} + C\frac{\partial^2\phi}{\partial\xi^2} = 0,$$

Using the tangent hyperbolic method, in the comoving frame of the nonlinear structure admits the following shock type solution.

$$\phi(\xi) = \frac{-25B+3C^2}{50AB} + \frac{3C^2}{25AB}\tanh\xi - \frac{3C^2}{50AB}\tanh^2\xi$$

As this solution satisfies the boundary conditions, so the value of C is taken as  $\sqrt{25B/6}$ .

#### A. Case A

For Carins distribution values of coefficients are found to be as,

$A = 0.5\left(\frac{1-\frac{v_+}{u}}{\Gamma-\frac{v_+}{u}}\right)$  And  $B = \left(\frac{-\rho_+^2}{\Gamma-\frac{v_+}{u}}\right)$ . Putting them in the solution, shock structures are obtained, which are illustrated in figures 11-14.

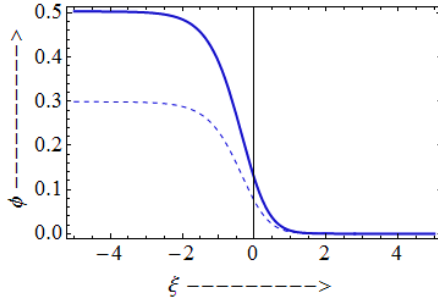


Fig.11. At Variation of the electrostatic drift potential  $\Phi$  with varying non-thermal ion population,  $\Gamma = 0.2$  (Thick) and  $\Gamma = 0.45$  (Dashed).

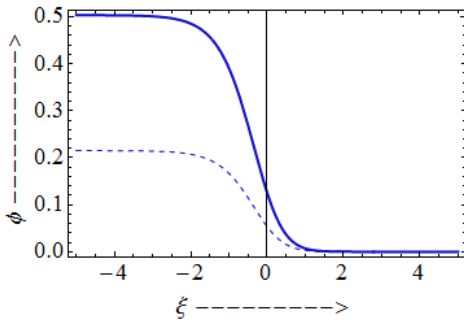


Fig.12. At Variation of the electrostatic drift potential  $\Phi$  with varying inverse scale length of density inhomogeneity  $\kappa_{ni} = 10^{-3}m$  (Thick) and  $\kappa_{ni} = .7 \times 10^{-3}m$  (Dashed).

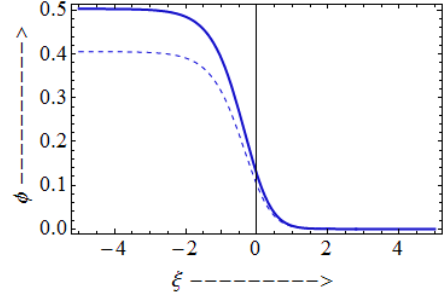


Fig.13. At Variation of the electrostatic drift potential  $\Phi$  with varying shock velocity  $u=180,000$  (Thick) and  $u=200,000$  (Dashed).

#### B. Case B

For kappa distribution values of coefficients are found to be as,

$A = 0.5\left(\frac{2\eta-\frac{v_+}{u}}{\Gamma-\frac{v_+}{u}}\right)$  And  $B = \left(\frac{-\rho_+^2}{\Gamma-\frac{v_+}{u}}\right)$ . Putting them in the solution, shock structures are obtained, which are illustrated in figures 14-16.

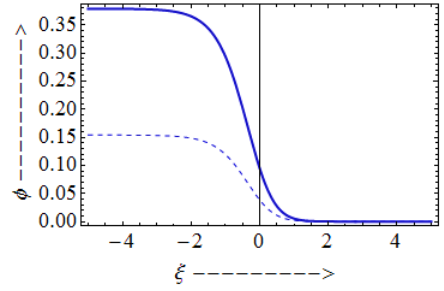


Fig.14. At Variation of the electrostatic drift potential  $\Phi$  with varying inverse scale length of density inhomogeneity  $\kappa_{ni} = 10^{-2}m$  (Thick) and  $\kappa_{ni} = .8 \times 10^{-3}m$  (Dashed).

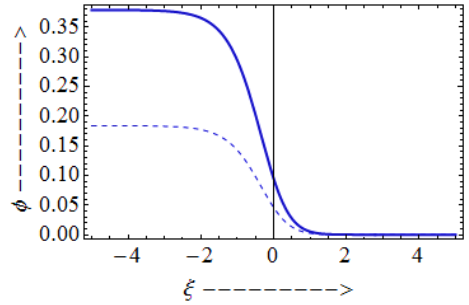


Fig.15. At Variation of the electrostatic drift potential  $\Phi$  with varying shock velocity  $u=25,000$  (Thick) and  $u=30,000$  (Dashed).

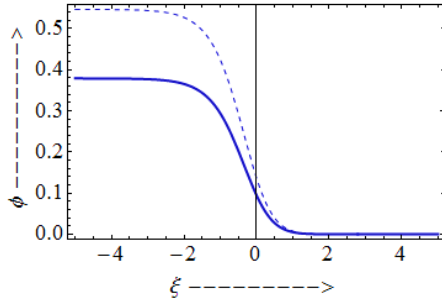


Fig.16. At Variation of the electrostatic drift potential  $\Phi$  with varying non-thermal ion population,  $\kappa = 2.8$  (Thick) and  $\kappa = 3$  (Dashed).

## II. OBSERVATIONS.

Since, it is seen from the solution that there is no contribution of magnetic field and ion collisional frequency, so any variation in these parameters will not vary the drift shock potential. Moreover by increasing inverse scale length of density inhomogeneity, nonthermal ion population and velocities, the drift shocks potentials are found to be increasing (figure 11 to 14) except for the case of kappa, where it is found to be decreasing as depicted in figure 16.

## III. CONCLUSION

In conclusion, numerical investigations have revealed the following, effects of varying ion-neutral collision frequency, non-thermal electron thermal population, inverse density inhomogeneity scale length, and the magnetic field strength varies nonlinear drift shock potential. The plasma parameters have been chosen that are typically found in the ionosphere's F-layer.<sup>16</sup> The value of the ion Larmor radius that moves with the ion acoustic speed,  $\rho_+$  for the chosen parameters turns out to be  $\sim 100$  cm. For Cairns distribution (fig.1-4), it is worth mentioning that the non-thermal electron population affects the drift shocks. Increase in above mentioned parameters changes the drift shock potential. On the other hand same procedure is revised with drift shock structures found by Kappa distribution (fig.5-8). It has been noticed that the strength of the drift shock potential is higher for Cairns by comparison with Kappa distribution. Scale lengths of drift shocks of Kappa distribution were found to be squeezed whereas shocks formed as a result of Cairns distributions are of larger scales in terms of their magnitudes and hence much stronger. Moreover, the KdVB drift shocks (Figure11-16) exclusively revealed that their strength is much stronger as more KP drift shocks. Since the variable  $\xi$  is normalized by  $\rho_+$ , therefore, the width of the shock turns out to be of the order of one tenth of a kilometer, whereas the width of the F2 layer is 220 – 800 km. Hence, we arrive at the conclusion that the shock formation in the F2 layer is possible.

Thus in the regions of space where so called “cavitons of plasma density” of Cairns non-thermal particle distribution recorded by Freja satellite are found, drift shocks are expected to be formed with different magnitudes and their strength can be varied depending on the associated parameters. Furthermore due to the presence of “accelerated suprathermal plasma density” of Kappa non-thermal distribution, first observed by Viking satellite and later others throughout in space, drift shocks of this genus may not be as strong but they are also expected to exist in those regions.

It is professed from the above exercise that the strength of the drift shock potential is highest for KdVB (Cairns). The spatial scale of the shock for the system under consideration turns out to be half a Kilometer.

## IV. ACKNOWLEDGMENT

This paper is an extension of work of Dr Waqas Masood *et al*<sup>1</sup>, and all the contents used (including the data and theoretical frame), are added under their permission.

## V. REFERENCES

- [1] Nonlinear electrostatic shock waves in inhomogeneous plasmas with nonthermal electrons, W. Masood, H. Rizvi, and H. Hasnain
- [2] N. S. Buchel’Nikova, R. A. Salimov, and I. Edelmak, Jr., Zh. Eksp. Teor. Fiz. 52, 837 (1967).
- [3] H. W. Hendel, T. K. Chu, and P. A. Politzer, Phys. Fluids 11, 2426 (1968).
- [4] V. P. Lakhin, A. B. Mikhailovskii, and O. G. Onishchenko, Phys. Lett. A.119, 348 (1987).
- [5] B. Sahu and R. Roychoudhury, Phys. Plasmas 14, 072310 (2007).
- [6] A. A. Mamun and P. K. Shukla, Phys. Plasmas 9, 1468 (2002).
- [7] J.-K. Xue, Phys. Plasmas 10, 4893 (2003).
- [8] [http://en.wikipedia.org/wiki/F\\_region](http://en.wikipedia.org/wiki/F_region)
- [9] Electro static solitary structures in non-thermal plasmas. R. A. Cairns, A.
- [10] Nonlinear Kinetic Alfvén waves with non-Maxwellian electron population in space plasmas . W.Masood, M . N. S. Qureshi, P. H. Yoon and H. A. Shah (2014)
- [11] Kappa distributions: theory and applications in space plasmas V. Pierrard and M. Lazar (2010)
- [12] P. K. Shukla and A. A. Mamun, New J. Phys. 5, 17 (2003).
- [13] The Tanh Method: A Tool to Solve Nonlinear Partial Differential Equations with Symbolic Software by Willy Hereman and Willy Malfliet
- [14] W. Malfliet, W. Hereman, The tanh method: I. Exact solutions of nonlinear evolution and wave equations, Physica Scripta 54, 563-568 (1996).
- [15] H. Tasso, Phys. Lett. A 24, 618 (1967).
- [16] Formation of solitary structures in uniform and nonuniform magnetoplasmas with superthermal electrons: a non-reductive perturbative approach by W. Masood, Sunia Hassan, N. Batool and M. Siddiq (2013).